



Density functional theory calculations for investigation of atomic structures of 4H-SiC/SiO₂ interface after NO annealing

Komatsu, Naoki
Ohmoto, Mizuho
Uemoto, Mitsuharu
Ono, Tomoya

(Citation)

Journal of Applied Physics, 132(15):155701

(Issue Date)

2022-10-21

(Resource Type)

journal article

(Version)

Version of Record

(Rights)

© 2022 Author(s). Published under an exclusive license by AIP Publishing.
This article may be downloaded for personal use only. Any other use requires prior permission of the author and AIP Publishing. This article appeared in Journal of Applied Physics 132, 155701 (2022) and may be found at...

(URL)

<https://hdl.handle.net/20.500.14094/0100477397>



Density functional theory calculations for investigation of atomic structures of 4H-SiC/SiO₂ interface after NO annealing

Cite as: J. Appl. Phys. **132**, 155701 (2022); <https://doi.org/10.1063/5.0102472>

Submitted: 10 June 2022 • Accepted: 19 September 2022 • Published Online: 18 October 2022

Naoki Komatsu, Mizuho Ohmoto,  Mitsuharu Uemoto, et al.



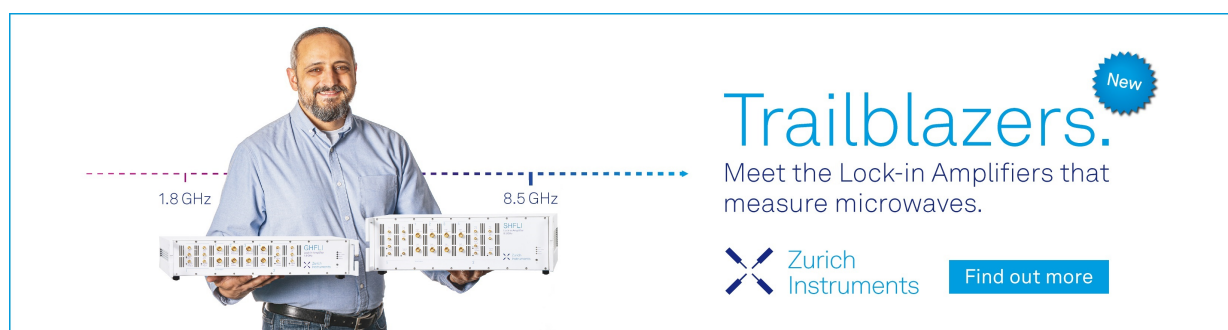
View Online




Export Citation




CrossMark



Trailblazers. 

Meet the Lock-in Amplifiers that measure microwaves.

 **Zurich Instruments** [Find out more](#)

Density functional theory calculations for investigation of atomic structures of 4H-SiC/SiO₂ interface after NO annealing

Cite as: J. Appl. Phys. **132**, 155701 (2022); doi: [10.1063/5.0102472](https://doi.org/10.1063/5.0102472)

Submitted: 10 June 2022 · Accepted: 19 September 2022 ·

Published Online: 18 October 2022



Naoki Komatsu, Mizuho Ohmoto, Mitsuharu Uemoto,  and Tomoya Ono^{a)} 

AFFILIATIONS

Department of Electrical and Electronic Engineering, Graduate School of Engineering, Kobe University, Nada, Kobe 657-8501, Japan

^{a)}Author to whom correspondence should be addressed: t.ono@eedept.kobe-u.ac.jp

ABSTRACT

We propose the atomic structures of the 4H-SiC/SiO₂ interface for *a* face (1 $\bar{1}$ 00), *m* face (11 $\bar{2}$ 0), the C face (000 $\bar{1}$), and Si face (0001) after NO annealing using the OH-terminated SiC surface models. Our proposed structures preferentially form at the topmost layers of the SiC side of the interface, which agrees with the experimental finding of secondary-ion mass spectrometry; that is, the N atoms accumulate at the interface. In addition, the areal N-atom density is of the order of 10¹⁵ atom/cm² for each plane, which is also consistent with the experimental result. Moreover, the electronic structure on the interface after NO annealing in which the CO bonds are removed and the nitride layer only at the interface is inserted, is free from gap states, although some interface models before NO annealing include the gap states arising from the CO bonds near the valence band edge of the bandgap. Our results imply that NO annealing can contribute to the reduction in the density of interface defects by forming the nitride layer.

Published under an exclusive license by AIP Publishing. <https://doi.org/10.1063/5.0102472>

I. INTRODUCTION

Silicon carbide (SiC) attracts attention because it is one of the most promising wide-bandgap semiconductors for developing next-generation switching devices operating in high-power and high-frequency applications.^{1–3} However, the potential of 4H-SiC has not been fully utilized owing to the low carrier mobility of 4H-SiC-based metal–oxide–semiconductor field-effect transistors, which is caused by defects at the 4H-SiC/SiO₂ interface. To reduce the density of interface defects and increase the channel mobilities, post-oxidation annealing using N₂O, NO, or N₂ gas has been proposed.^{4–8} In previous studies for the experimental characterizations of the annealed SiC/SiO₂ interface, the incorporated N atoms were fixed at the C-atom sites of the SiC substrate side, which were chemically bonded with Si atoms.^{9,10} The presence of a high-N-atom-density layer, which is hereafter called the nitride layer, was observed by the secondary-ion mass spectrometry of the *a* face (1 $\bar{1}$ 00), *m* face (11 $\bar{2}$ 0), Si face (0001), and C face (000 $\bar{1}$). Since the N-atom density is on the order of 10¹⁴–10¹⁵ atom/cm² for each crystal plane,^{10,11} it is expected that most of the C atoms at

the interface are substituted by N atoms. On the basis of their low-energy electron diffraction measurements, Shirasawa *et al.* proposed a model of the N-annealed 6H-SiC/SiO₂ interface, which constitutes epitaxially stacked SiO₂ and Si₃N₂ monolayers (SiON) on SiC.^{12,13} A similar structure was also determined for 4H-SiC using the simulated x-ray absorption spectroscopy spectrum.¹⁴ Moreover, some experiments reported that the N-atom density after annealing is different depending on the crystal planes. The N nuclear reaction analysis of the 4H-SiC/SiO₂ interface showed that the concentration of N atoms on the *a* face is more than twice that of the Si face. Hamada *et al.*¹⁰ reported that the *m* face has nearly the same concentration of N atoms as the *a* face. Regardless of the annealing temperature, N-atom incorporation occurs in the order of $a \approx m \ll \text{Si}$, excluding the C face. Although the anisotropy mechanism has been investigated so far, the atomic-scale structures of the interface after annealing have been unclear for arbitrary crystal planes. In our previous study,¹⁵ we proposed the interface atomic structures in which N atoms are incorporated by replacing C atoms, and we investigated the total energies and electronic structures of the nitride layers by density functional theory (DFT) calculation.¹⁶

It was found that the incorporation at the k site on the a face is energetically most stable, and the areal density of N atoms in our model ($\approx 10^{15}$ atom/cm²) agrees well with experimental results. However, the previous study employed the models where the nitride layers form in a SiC bulk and the interaction between the substrate and oxides is not considered.

In this study, we employ the interface models in which the atomic structures include oxides to investigate the effects of the interaction between the substrate and oxides. Universal atomic-scale models describing 4H-SiC with a high-N-atom-density layer in arbitrary crystal planes are proposed. To explore the most preferable crystal plane of 4H-SiC for N-atom incorporation by NO annealing, we study the stability and electronic states of the nitride layers on a 4H-SiC surface. We find that the nitride layers grow along the a face, which is consistent with the conclusion obtained using the bulk model,¹⁵ and NO bonds are hardly generated at the interface. Any defect states in the bandgap of 4H-SiC are not generated in our structure after N-atom incorporation. The formation energy of the nitride layers at the topmost layer of the interface is smaller than that at the second layer, indicating that the N atoms accumulate at the interface. Although some of our models do not contain SiO₂ layers on the SiC substrate, we assured that our conclusions are not affected when the SiO₂ layers are attached on the substrate.

The rest of this paper is organized as follows. Section II is devoted to the description of the methods used in this work. In Sec. III, we propose the interface atomic structures after N-atom incorporation and consider the formation energies of the proposed structures. The conclusions are drawn in Sec. IV.

II. METHOD

In our model, the surface of the 4H-SiC substrate is terminated with hydroxy groups to imitate the SiO₂ layer, and the other side of the substrate is terminated with H atoms. Although the SiO₂ on the SiC substrate is amorphous, it is not easy to discuss the stability of the atomic structures using a few interface models. Therefore, the simplified interface models are employed in this study. As introduced in the [supplementary material](#), the conclusion is not affected when SiO₂ layers are formed on the substrate. We employ rectangular supercells of $10.1 \times 5.3 \times 26.3 \text{ \AA}^3$ for the a -face model, $10.1 \times 6.2 \times 27.3 \text{ \AA}^3$ for the m -face model, and $6.2 \times 5.3 \times 26.8 \text{ \AA}^3$ for the Si(C)-face model. The direction perpendicular to the surface is taken to be the z axis. At the interface, two types of interface atomic structure are prepared, where CO bonds are present in one type and are absent in the other type. The number of atoms for the a -face, m -face, and Si(C)-face models are 88, 104, and 52, respectively, and the numbers are not affected by the presence of the CO bonds. [Figures 1 and 2](#) show the interface atomic structures before N-atom incorporation without and with the CO bonds, respectively. Although it remains to be clarified whether the inserted N atoms exist at the SiO₂ side or the SiC side of the interface, we assume that the N atoms accumulate at the SiC side on the basis of the possibility proposed in the previous experimental studies.^{10,11} From the similarity of the SiON layer model reported by Shirasawa *et al.*,^{12,13} stable structures without dangling bonds are required. In our previous study,¹⁵ we set up the atomic structures after N-atom incorporation using the experimental

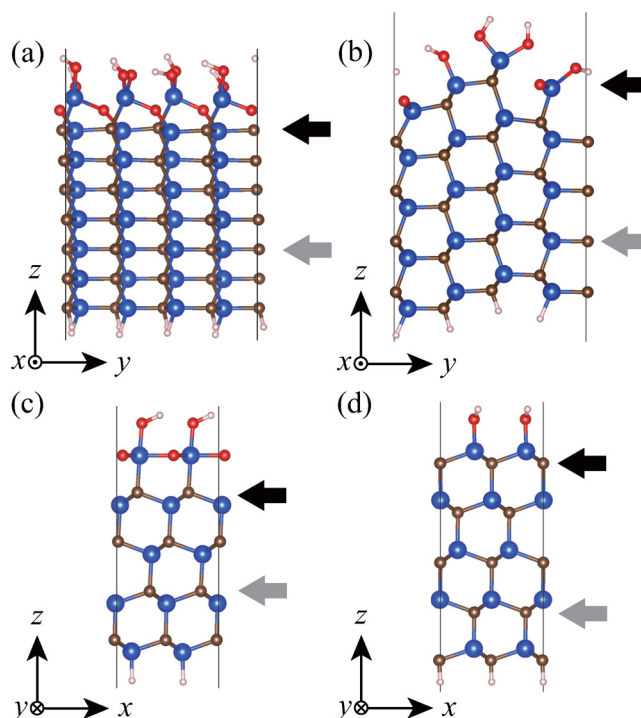


FIG. 1. Interface atomic structures without CO bonds for (a) a -, (b) m -, (c) C-, and (d) Si-face models before N-atom incorporation. Blue, brown, red, and gray spheres are Si, C, O, and H atoms, respectively. Black lines are the boundaries of the supercell.

results obtained secondary-ion mass spectrometry, x-ray absorption spectroscopy, and x-ray emission spectroscopy.^{9–14} Then, we proposed the modification incorporating one Si vacancy (V_{Si}) and 4 N atoms at C sites (N_C s). In our previous study, it was found that the lattice constant mismatch between the SiC substrate and nitride layers is less than 2%. The arrangement of the V_{Si} s in the crystal planes and the position of the V_{Si} s in the two inequivalent lattice sites of 4H-SiC, i.e., h (hexagonal) and k (quasi-cubic) sites, have been investigated in Ref. 15. The most stable atomic structures are with N-atom incorporation in which V_{Si} s are arranged at the linear alignment and the k sites are employed in this study. Although the interface with CO bonds does not contain SiO₂ layers on the SiC substrate, the O atoms of hydroxy groups are positioned so as to imitate O atoms in SiO₂. [Figures 3 and 4](#) show the interface atomic structures with the nitride layers for the interfaces without and with the CO bonds, respectively. The areal N-atom densities in the present models are 1.48×10^{-15} , 1.29×10^{-15} , 1.22×10^{-15} , and 1.22×10^{-15} atoms/cm² for a , m , C, and Si faces, respectively, while the areal C-atom densities at the top layer are 9.98×10^{-14} , 6.47×10^{-14} , 1.22×10^{-15} , and 1.22×10^{-15} atoms/cm² for a , m , C, and Si faces, respectively. Therefore, most of the C atoms are substituted by N atoms at the interface. The interfaces with the nitride layer at the second layer are also investigated for all the faces. For the DFT calculation, we employ the RSPACE code,^{17–20} which

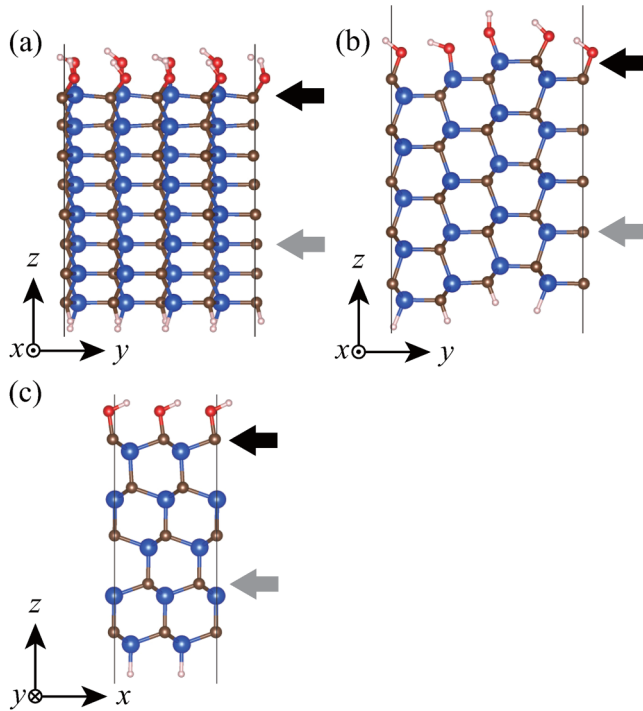
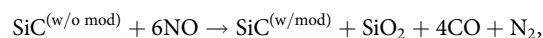


FIG. 2. Interface atomic structures with CO bonds for (a) *a*-, (b) *m*-, and (c) C-face models before N-atom incorporation. The meanings of the symbols are the same as those in Fig. 1.

uses the real-space finite-difference approach^{21,22} within the frameworks of DFT.¹⁶ The local density approximation²³ of the DFT is used to describe the exchange and correlation effects.²⁴ The projector-augmented wave method is used for electron-ion interactions.²⁵ We adopt $6 \times 12 \times 1$, $12 \times 6 \times 1$, and $12 \times 12 \times 1$ Monkhorst-pack *k*-point meshes, including a Γ -point in the Brillouin zone for the *a*-face, the *m*-face, and the Si(C)-face models, respectively. The real-space grid spacing is chosen to be ≈ 0.21 Å. The structural optimization is performed until the residual forces are smaller than 0.001 Hartree/Bohr radius.

III. RESULTS AND DISCUSSION

The assumed interaction of the SiC substrate and the arriving NO molecule at the interface is expressed as



with $\text{SiC}^{(\text{w/o mod})}$ ($\text{SiC}^{(\text{w/mod})}$) being the interface without (with) the modification incorporating one V_{Si} and four N_{C} s. The formation energy of the above interaction for generating one modification is obtained as

$$E_{\text{form}} = E_{\text{total}}^{(\text{w/mod})} / n + E(\text{SiO}_2) + 4\mu_{\text{CO}} + 2\mu_{\text{N}} - E_{\text{total}}^{(\text{w/o mod})} / n - 6\mu_{\text{NO}}, \quad (1)$$

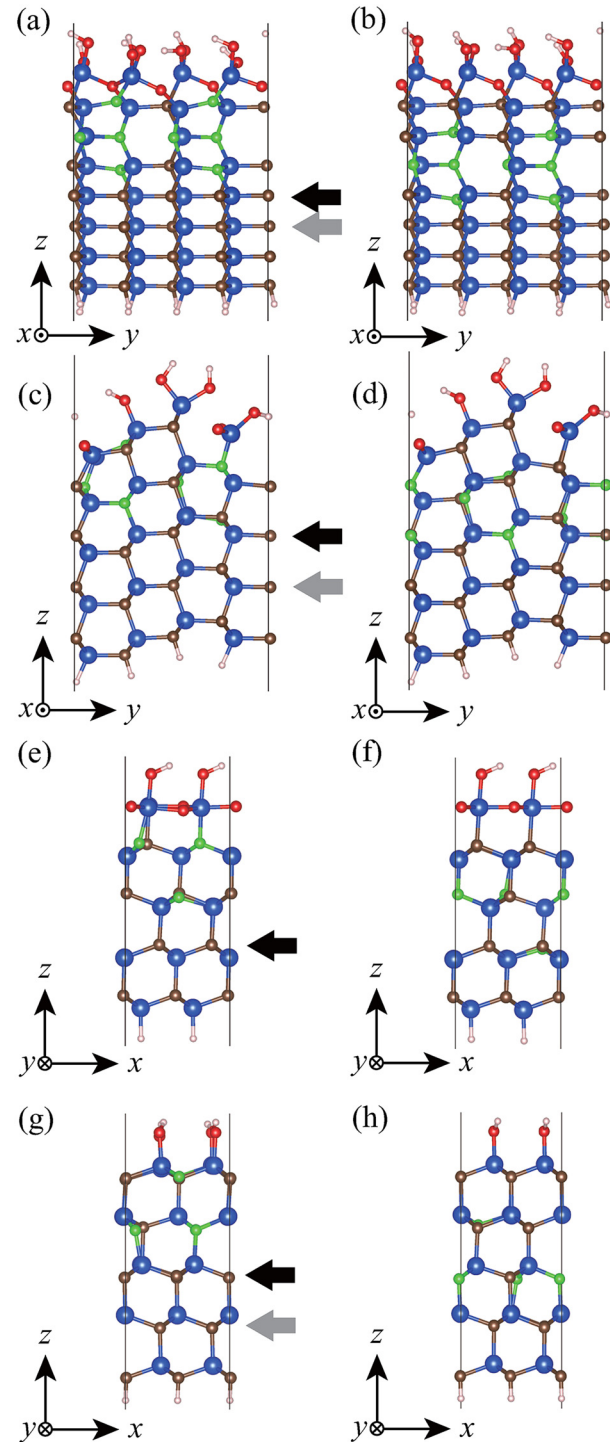


FIG. 3. Interface atomic structures without CO bonds for (a) [(b)] *a*-, (c) [(d)] *m*-, (e) [(f)] C-, and (g) [(h)] Si-face models with nitride layers at the topmost (second) bilayer. Green spheres are N atoms. The meanings of the other symbols are the same as those in Fig. 1.

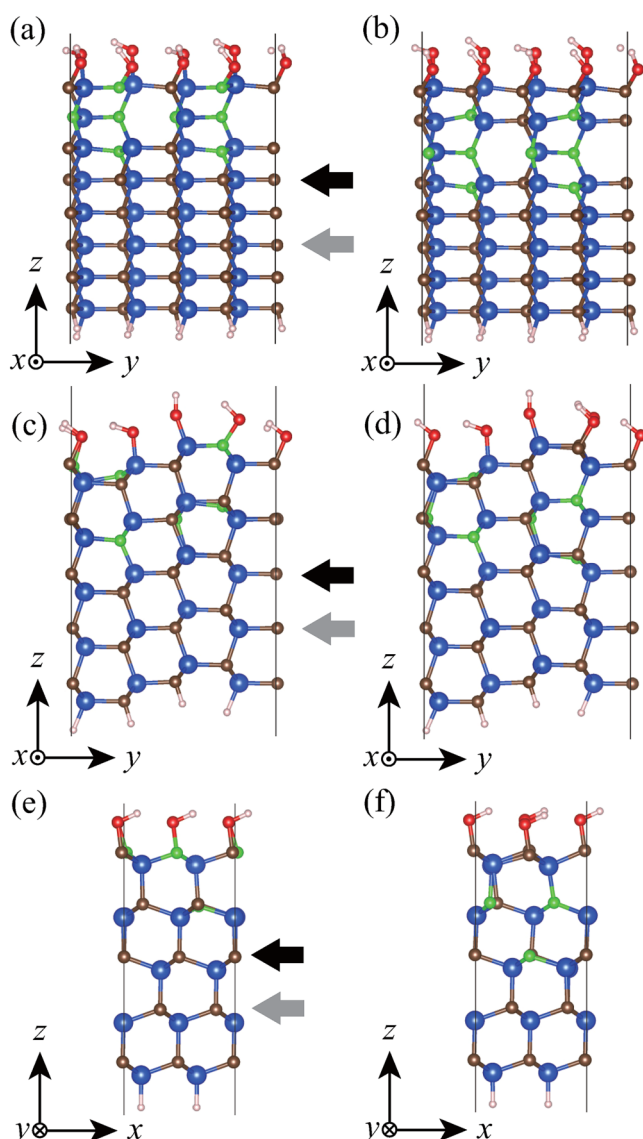


FIG. 4. Interface atomic structures with CO bonds for (a) [(b)] *a*-, (c) [(d)] *m*-, and (e) [(f)] *C*-face models with nitride layers at the topmost (second) bilayer. The meanings of the symbols are the same as those in Fig. 3.

where $E(\text{SiO}_2)$ is the total energy of a SiO_2 unit in a bulk of quartz SiO_2 , $E_{\text{total}}^{(\text{w/o mod})}$ ($E_{\text{total}}^{(\text{w/mod})}$) represents the total energy of the interface without (with) N-atom incorporation, and n is the number of modifications introduced in a supercell. According to the lateral length of the supercell, n is set to be 2 for the *a*-face and *m*-face models, while n is 1 for the *C*-face model. In addition, μ_{NO} , μ_{CO} , and μ_{N} are the chemical potentials of a NO molecule, a CO molecule, and N atoms in a N_2 molecule, respectively. The chemical potential for the N atom at temperature T is

determined as

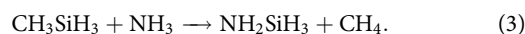
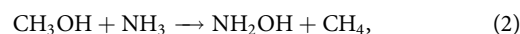
$$\mu_{\text{N}}(T, p_{\text{N}_2}) = \mu_{\text{N}_2}(T, p^0) + \frac{1}{2} k_B T \ln \left(\frac{p_{\text{N}_2}}{p^0} \right),$$

$$\mu_{\text{N}_2}(T, p^0) = \mu_{\text{N}_2}(0\text{K}, p^0) + \frac{1}{2} \Delta G_{\text{N}_2}(T, p^0),$$

with k_B and G being the Boltzmann constant and Gibbs's free energy, respectively. $\mu_{\text{N}_2}(0\text{K}, p^0)$ at $p^0 (=1 \text{ atm})$ is the total energy of the N_2 molecule computed by DFT using a supercell containing a sufficiently large vacuum region. The thermochemical parameters for Gibbs's free energy are taken from Ref. 26. The chemical potentials for NO and CO molecules are calculated in a similar manner. We set the temperature at 1000 K and the partial pressure of the NO gas (p_{NO}) at 1 atm. Since the annealing process is not in an equilibrium state, it is not straightforward to determine the partial pressures of CO (p_{CO}) and N_2 (p_{N_2}) gases. Here, p_{CO} (p_{N_2}) is varied between 10^{-1} and 10^{-5} atm (0.25×10^{-1} and 0.25×10^{-5} atm).

The formation energies of the nitride layers with respect to p_{CO} and p_{N_2} are shown in Fig. 5. It is found that the reactions are exothermic, and the nitride layers growing along the *a* face are the most stable ones among those along the *a*, *m*, *C*, and *Si* faces. Although SiO_2 layers are absent in some models, this trend does not change when SiO_2 layers are attached as shown in the supplementary material. In addition, these results are consistent with the conclusion obtained for the nitride layers in bulk; that is, the nitride layer preferentially grows along the *a* face from the viewpoint of thermodynamics,¹⁵ and the dependence of the areal N-atom density on the crystal plane reported in Ref. 10 is caused by the kinetic factor. In the case of the interfaces without the CO bonds, the formation energy of the nitride layer at the topmost layer is smaller than that at the second layer, resulting in the localization of the N atoms at the interface. The difference in the formation energy between the nitride layers at the topmost and second layers is the largest for the *a* face. This result agrees well with the observation that the atomically flat nitride layers grow along the *a* face.

In the case of the interfaces with the CO bonds, compared with the interfaces with the nitride layer at the topmost and second layers, we find that the formation of the nitride layer at the second layer is stable. When the nitride layers are generated at the topmost layer, the C atoms connected to O atoms are replaced by N atoms. However, the formation of NO bonds is not more preferable than that of the SiN bonds. To ensure the stability of the SiN bonds over the NO bonds, we examine the following interactions with isolated molecules:



The reaction energy is defined as the total energy of the right hand side subtracted by that of the left hand side. The reaction energy of the interaction [Eq. (2)] is 0.44 eV, while that of Eq. (3) is -0.17 eV. Among Si, C, N, and O atoms, the electronegativity of a Si atom is the smallest and Si atoms are positively charged at the

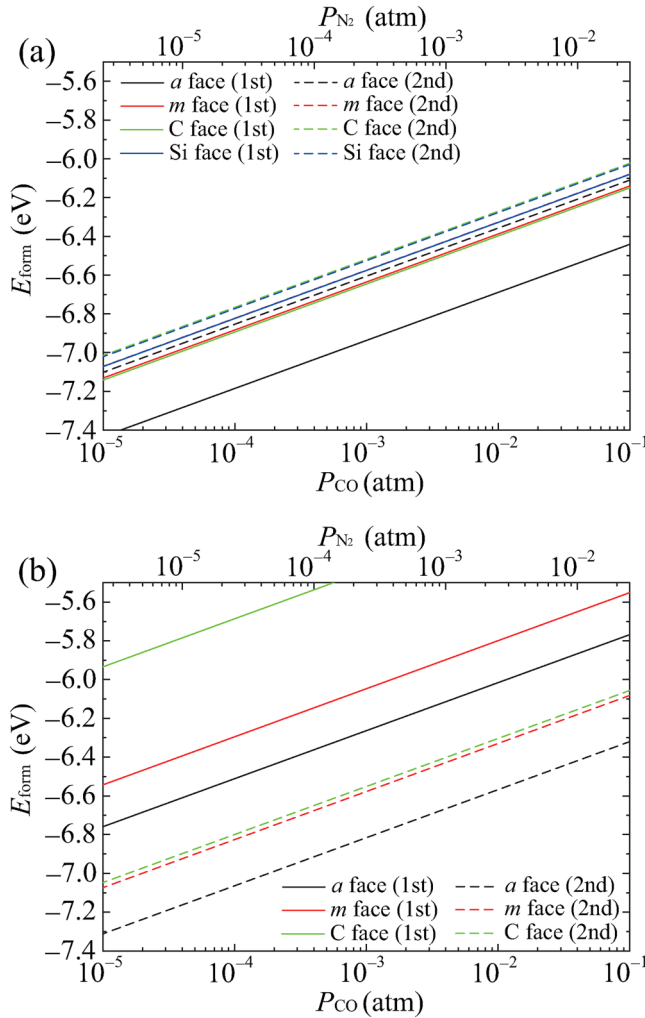
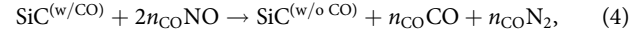


FIG. 5. Formation energies E_{form} defined Eq. (1) for interface (a) without and (b) with CO bonds with respect to partial pressures of CO and N_2 .

SiC/SiO_2 interface. Therefore, the bonds with positively charged Si and negatively charged N atoms are stable, resulting in the stabilization of the atomic structure with the nitride layer at the second layer. The difference in the formation energy between the nitride layers at the topmost and second layers of the C face is significantly larger than those of the other faces. This is because the number of NO bonds generated by the formation of the nitride layer is the largest in the case of the C face.

The interface atomic structure where the nitride layer exists at the second layer contains the transition layer between the SiO_2 and nitride layers. It is counterintuitive that a V_{Si} is formed directly at the second layer. The DFT calculation using the nudged energy band method reveals that the energy barrier of V_{Si} from the topmost layer to the second layer along the (0001) direction is ≈ 5.0 eV, indicating that the migration of V_{Si} hardly occurs at the

interface. Then, we consider the interactions between NO molecules and the interface with the CO bonds, which are the source of the transition layer. The interactions are expressed as



where $\text{SiC}^{(\text{w/o CO})}$ and $\text{SiC}^{(\text{w CO})}$ are the interfaces without and with the CO bonds shown in Figs. 1 and 2, respectively, and n_{CO} is the number of CO bonds in a supercell. n_{CO} is 8 for the a-face and m-face models and is 16 for the Si(C)-face model. The formation energy of the reaction [Eq. (4)] is defined as

$$E_{\text{form}} = E_{\text{total}}^{(\text{w/o CO})}/n_{\text{CO}} + \mu_{\text{CO}} + 2\mu_{\text{N}} - E_{\text{total}}^{(\text{w CO})}/n_{\text{CO}} - 2\mu_{\text{NO}}, \quad (5)$$

where $E_{\text{total}}^{(\text{w/o CO})}$ ($E_{\text{total}}^{(\text{w CO})}$) is the total energy of the interface with (without) the CO bonds and p_{CO} and p_{N_2} are varied between 10^{-1} and 10^{-5} atm. Figure 6 shows the formation energy for the elimination of the CO bonds at the interface. We find that all the reactions are exothermic, indicating that the CO bonds are removed before N-atom incorporation, the NO bonds are hardly generated at the interface, and the transition layer is absent even when the CO bonds exist before N-atom incorporation. Thus, the NO annealing generates the nitride layers immediately below the SiO_2 layers without any transition layers.

Finally, we show in Fig. 7 the local density of states (LDOS) of the interface before and after N-atom incorporation. The LDOS is calculated as

$$\rho(z, E) = \sum_{i,k} \int |\Psi_{i,k}(x, y, z)|^2 dx dy \times N e^{-\alpha(E - \varepsilon_{i,k})^2},$$

where $\varepsilon_{i,k}$ are the eigenvalues of the wavefunction with indexes i and k denoting the eigenstate and the k -point, respectively, z is the

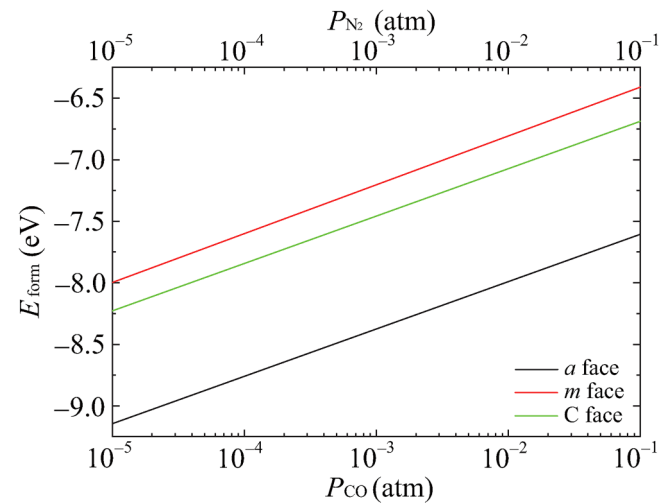


FIG. 6. Formation energies E_{form} defined Eq. (5) for interface without CO bonds from that with CO bonds with respect to partial pressures of CO and N_2 .

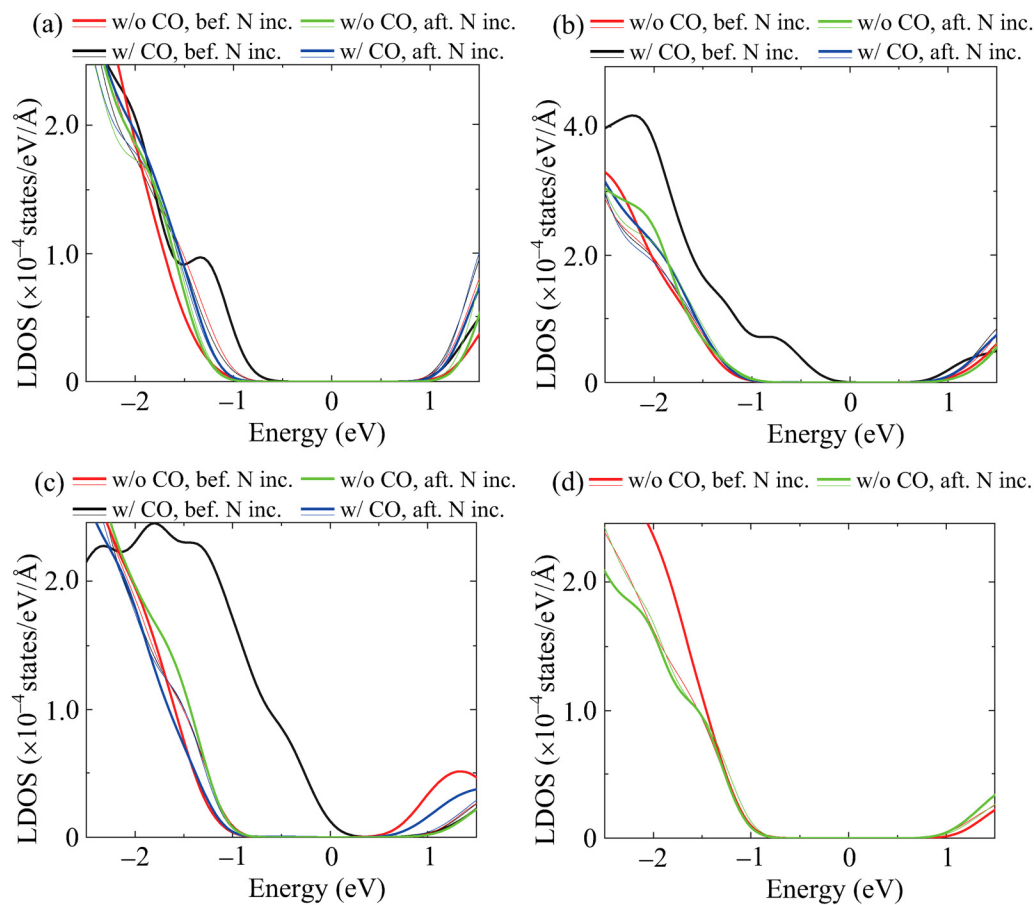


FIG. 7. LDOS for (a) *a*-, (b) *m*-, (c) *C*-, and (d) *Si*-face models. Red and black (green and blue) curves indicate the LDOS before (after) N-atom incorporation. Red and green (black and blue) curves are the LDOS for the interface models without (with) the CO bonds. Thick curves are the LDOS on the planes indicated by black arrows in Figs. 1–4, while thin curves are the LDOS on the planes indicated by gray arrows.

coordinate of the plane where the LDOS is plotted, and $N(=2\sqrt{\frac{\pi}{\alpha}})$ is the normalization factor with α as the smearing factor. Here, α is set to 13.5 eV^{-2} . The LDOS at the interface is plotted on the plane, which includes the topmost C atom of the SiC substrate, while the plane for the bulk is chosen to be far from the interface so that the interactions between the SiO₂ and nitride layers are eliminated. The planes for the interfaces and those for the bulks are indicated by the black and gray arrows, respectively, in Figs. 1–4. The bandgaps are underestimated due to the usage of the local density approximation and are enlarged by the finite-size effect of the slab models. The LDOS is shifted so that the center of the bandgap of the LDOS in the bulk corresponds to zero energy. It is found that the states arising from the CO bonds lie near the valence band edge of the bandgap in all the models with the CO bonds before N-atom incorporation. Although the hydroxy groups are directly attached to the SiC substrate in the case of the structures with CO bonds, we assured that the existence of SiO₂ layers does not affect the existence of the states due to the CO bonds in

the [supplementary material](#). The effect of the CO bonds is significant at the C face; we confirm that this effect survives even when the thickness of the oxide layer is increased. The gap states at the topmost layer of the SiC side of the interface disappear by introducing the nitride layer between the SiC substrate and the SiO₂ layer, indicating that the N-atom incorporation by NO annealing can contribute to the reduction in the density of interface defects.

IV. CONCLUSION

The DFT calculations were carried out to investigate the electronic structures and stability of the 4H-SiC/SiO₂ interface after NO annealing using the OH-terminated SiC surface models and the assumption derived from the experiments^{10,11} that the N atoms are fixed at the C-atom site of the SiC. We found that N-atom incorporation by NO annealing, in which four C atoms adjacent to the V_{Si} are replaced by N atoms, is an exothermic reaction, and the formation energy for the nitride layer growing along the *a* face is the smallest, even when the models containing oxides are

employed, indicating that the dependence of the areal N-atom density on the crystal plane is induced by the kinetic factors during the reaction rather than thermodynamic factors. In addition, in the case of the interface without the CO bonds, the nitride layer at the topmost layer of the interface is more stable than that at the second bilayer, resulting in the formation of the nitride layers at the topmost layer of the interface. We also investigated the interfaces in which the CO bonds remain after the thermal oxidation. Although the CO bonds at the interface prevent the generation of the nitride layer at the topmost layer of the SiC side, the CO bonds are removed before N-atom incorporation because the reaction between the CO bonds and NO molecules is exothermic. From these results, it is reasonable to conclude that NO annealing forms the nitride layers immediately below the SiO₂ layers without any transition layers. LDOS analysis revealed that the states relevant to the CO bonds at the interface lie near the valence band edge of the bandgap in all the interface models. On the other hand, there are no gap states in the interface after N-atom incorporation. These results imply that NO annealing after the oxidation can contribute to the reduction in the density of interface defects by forming the nitride layer immediately below the SiO₂ layer of the interface.

SUPPLEMENTARY MATERIAL

See the [supplementary material](#) for additional data when the SiO₂ layers are attached to the SiC substrate.

ACKNOWLEDGMENTS

This work was partially financially supported by the MEXT as part of the “Program for Promoting Researches on the Supercomputer Fugaku” (Quantum-Theory-Based Multiscale Simulations toward the Development of Next-Generation Energy-Saving Semiconductor Devices, No. JPMXP1020200205), JSPS KAKENHI (No. JP16H03865), Kurata Grants, and the Iwatani Naoji Foundation. The numerical calculations were carried out using the computer facilities of the Institute for Solid State Physics at the University of Tokyo, the Center for Computational Sciences at the University of Tsukuba, and the supercomputer Fugaku provided by the RIKEN Center for Computational Science (Project ID hp210170).

AUTHOR DECLARATIONS

Conflict of Interest

The authors have no conflicts to disclose.

Author Contributions

Naoki Komatsu: Conceptualization (equal); Data curation (equal); Formal analysis (equal); Investigation (equal); Supervision (lead). **Mizuho Ohmoto:** Data curation (equal); Formal analysis (equal); Investigation (equal). **Mitsuharu Uemoto:** Data curation (equal);

Formal analysis (equal); Investigation (equal); Validation (equal). **Tomoya Ono:** Conceptualization (equal); Investigation (equal); Supervision (lead); Validation (equal).

DATA AVAILABILITY

The data that support the findings of this study are available from the corresponding author upon reasonable request.

REFERENCES

- ¹H. Okumura, *Jpn. J. Appl. Phys.* **45**, 7565 (2006).
- ²T. Kimoto, *Jpn. J. Appl. Phys.* **54**, 040103 (2015).
- ³T. Kimoto and H. Watanabe, *Appl. Phys. Exp.* **13**, 120101 (2020).
- ⁴H.-F. Li, S. Dimitrijević, H. B. Harrison, and D. Sweatman, *Appl. Phys. Lett.* **70**, 2028 (1997).
- ⁵G. Y. Chung, C. C. Tin, J. R. Williams, K. McDonald, M. Di Ventura, S. T. Pantelides, L. C. Feldman, and R. A. Weller, *Appl. Phys. Lett.* **76**, 1713 (2000).
- ⁶H. Yoshioka, T. Nakamura, and T. Kimoto, *J. Appl. Phys.* **112**, 024520 (2012).
- ⁷P. Fiorenza, F. Giannazzo, and F. Roccaforte, *Energies* **12**, 2310 (2019).
- ⁸T. Masuda, T. Hatakeyama, S. Harada, and H. Yano, *Jpn. J. Appl. Phys.* **58**, SBBD04 (2019).
- ⁹R. Kosugi, T. Umeda, and Y. Sakuma, *Appl. Phys. Lett.* **99**, 182111 (2011).
- ¹⁰K. Hamada, A. Mikami, H. Naruoka, and K. Yamabe, *e-J. Surf. Sci. Nanotechnol.* **15**, 109 (2017).
- ¹¹S. Dhar, L. C. Feldman, K.-C. Chang, Y. Cao, L. Porter, J. Bentley, and J. Williams, *J. Appl. Phys.* **97**, 074902 (2005).
- ¹²T. Shirasawa, K. Hayashi, S. Mizuno, S. Tanaka, K. Nakatsuji, F. Komori, and H. Tochiwara, *Phys. Rev. Lett.* **98**, 136105 (2007).
- ¹³T. Shirasawa, K. Hayashi, H. Yoshida, S. Mizuno, S. Tanaka, T. Muro, Y. Tamenori, Y. Harada, T. Tokushima, Y. Horikawa, E. Kobayashi, T. Kinoshita, S. Shin, T. Takahashi, Y. Ando, K. Akagi, S. Tsuneyuki, and H. Tochiwara, *Phys. Rev. B* **79**, 241301 (2009).
- ¹⁴N. Isomura, K. Kutsuki, K. Kataoka, Y. Watanabe, and Y. Kimoto, *J. Synchrotron Radiat.* **26**, 462 (2019).
- ¹⁵M. Uemoto, N. Komatsu, Y. Egami, and T. Ono, *J. Phys. Soc. Jpn.* **90**, 124713 (2021).
- ¹⁶P. Hohenberg and W. Kohn, *Phys. Rev.* **136**, B864 (1964).
- ¹⁷T. Ono and K. Hirose, *Phys. Rev. Lett.* **82**, 5016 (1999).
- ¹⁸T. Ono and K. Hirose, *Phys. Rev. B* **72**, 085115 (2005).
- ¹⁹K. Hirose, T. Ono, Y. Fujimoto, and S. Tsukamoto, *First-Principles Calculations in Real-Space Formalism, Electronic Configurations and Transport Properties of Nanostructures* (Imperial College, London, 2005).
- ²⁰T. Ono, M. Heide, N. Atodiresei, P. Baumeister, S. Tsukamoto, and S. Blügel, *Phys. Rev. B* **82**, 205115 (2010).
- ²¹J. R. Chelikowsky, N. Troullier, and Y. Saad, *Phys. Rev. Lett.* **72**, 1240 (1994).
- ²²J. R. Chelikowsky, N. Troullier, K. Wu, and Y. Saad, *Phys. Rev. B* **50**, 11355 (1994).
- ²³S. H. Vosko, L. Wilk, and M. Nusair, *Can. J. Phys.* **58**, 1200 (1980).
- ²⁴We have also adopted the generalized gradient approximation for similar systems in Ref. 15 and found that the conclusion is not changed by the exchange-correlation functional.
- ²⁵P. E. Blöchl, *Phys. Rev. B* **50**, 17953 (1994).
- ²⁶M. W. J. Chase, *NIST-JANAF Thermochemical Tables*, 4th ed. (AIP, 1998).